Optica Applicata, Vol. XXXII, No. 3, 2002

Designing guidelines for nitride VCSELs resonator

PAWEŁ MAĆKOWIAK, MICHAŁ WASIAK, TOMASZ CZYSZANOWSKI, ROBERT P. SARZAŁA, WŁODZIMIERZ NAKWASKI

Institute of Physics, Technical University of Łódź, ul. Wólczańska 219, 93–005 Łódź, Poland.

The main goal of this work is to present designing processes of nitride VCSELs taking into consideration technological difficulties in their manufacturing and complexity of their structures. We performed numerical simulations of possible nitride VCSELs. The analysis was carried out using an advanced 3D thermal-electrical-optical self-consistent modelling. We suggest some optimal configurations of distributed Bragg reflectors (DBRs) as well as active region composition, dimensions and localization. We also analyse difficulties associated with an efficient current confinement and carrier injection into the active region. Besides, our considerations cover the application of a tunnel junction and a semitransparent contact in nitride VCSELs.

1. Introduction

Nitride vertical-cavity surface-emitting lasers (VCSELs) emitting in the blue and ultraviolet wavelength ranges are very promising candidates for full-color displays, chemical sensing, high-density optical storage applications and high-resolution printing industry in view of low divergence of their output beams and the possibility of fabricating dense two-dimensional arrays. Edge-emitting nitride lasers are already commercially available, while electrically pumped nitride VCSELs have not been reported until now at all. The main obstacle for their successful construction is the confinement of an efficient current and carrier injection into the active region.

This paper presents technological difficulties and complexity of designing processes associated with nitride VCSELs. We try to give explanation why nitride VCSELs have not been manufactured yet. To answer that question we performed numerical simulations of possible nitride VCSEL configurations. The continuous -wave (CW) room-temperature (RT) analysis was carried out with the aid of an advanced 3D thermal-electrical-optical self-consistent simulation. Our model is based on the effective frequency method and the parabolic band-gap approximation in the optical part and the finite element method in the thermal, as well as in the electrical parts. The model with detailed assumptions and the material parameters are explained elsewhere [1]–[4].

A VCSEL resonator usually consists of two distributed Bragg reflectors (DBRs) and the active region placed properly between them in an anti-node of a standing wave. The active region is also sandwiched by so-called spacers. In arsenide or phosphide VCSELs at least one mirror is electrically conductive, so the current can

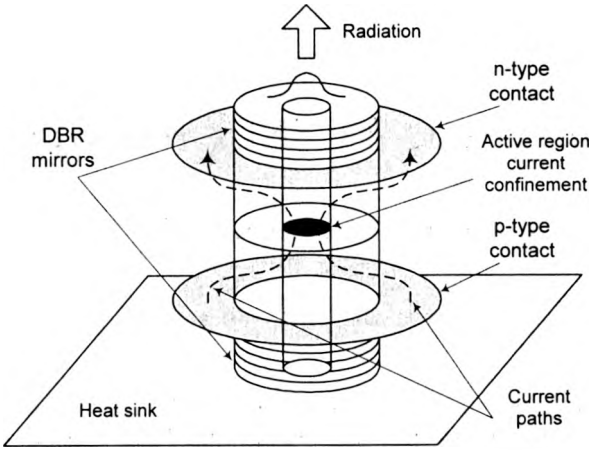

Fig. 1. Scheme of double lateral injection in a traditional VCSEL.

easily reach the active layer. Unfortunately, nitride DBRs are of a very poor electrical conductivity and the current has to be laterally injected into the active region (*cf.* Fig. 1). Additionally, due to the difference in the length of emitted radiation, a nitride resonator is much shorter than that of arsenide or phosphide VCSELs. Thus Joule heat generation associated with lateral currents is much higher in nitrides (especially of p-type). There is also no easy way to fabricate current confinement in nitrides as it is in the case of arsenide lasers where lateral oxidation of AlAs layer could be employed to form both carrier and optical confinement. Therefore, completely new designing approach needs to be applied to construct electrically pumped nitride VCSEL.

In the following sections some designing guidelines are discussed. To enable comparison between different considered structures we established a following standard set of parameters common in all designs. The desired emission wavelength is assumed to be 400 nm. All the layers between the bottom and the top DBR resonator mirrors comprise a 3λ cavity. The active region is the one analysed by PARK *et al.* [5], so it is composed of $In_{0.15}Ga_{0.85}N$ quantum well layer sandwiched by $In_{0.02}Ga_{0.98}N$ barriers. An active region radius is initially assumed to be 5 μm. For simplicity, step gain profile is assumed in the calculations. The reasons behind these choices are explained in the following sections.

2. DBR mirrors

To enable an epitaxial growth of an active layer, a DBR mirror close to the substrate ought to have the lattice constant similar to that of an active layer. Thus the natural choice for a bottom DBR mirror are nitride materials. Although the AlN/GaN [6] mirrors may ensure high refractive index step, the lattice constant of AlN substantially differs from that of GaN. Therefore, there is a need to introduce intermediate strain relief layers in the AlN/GaN DBRs or to use AlGaN instead of

AlN [7]. In the latter case, however, the refractive index step is lower, which results in the increasing number of periods of a DBR. What is worse, AlN and AlGaN layers (especially of p-type) are of very low electrical conductivity, which hinders an efficient electrical injection into the active region. There are not many solutions to this problem. One is to apply the lift-off technique [8] to separate the substrate from the active region and to use dielectric mirrors on both sides of the active layer [9]. This implies intra-cavity contacts and a double lateral carrier injection scheme with additional technological difficulties. Besides, dielectric mirrors are of low thermal conductivity, hence heat extraction in CW operating devices could be very inefficient. There is also a possibility to use a fusion bonding technique [10] to replace dielectric mirrors with electrically conductive ones. The bonding would take place between semiconductors of completely different lattice constants, which requires the development of an adequate technique for nitride materials and is currently unachievable. One could also consider a metallic mirror, but reflectivity of such mirrors are less than 96%, which is considerably too little for a VCSEL (to efficiently compensate these losses, the active region would have to supply extremely high optical gain).

Assuming that the gain in a typical InGaN active region is about 6000 cm^{-1}, and that only 3 to 5 quantum wells (3.5 nm each) can contribute to the gain, we calculate an amplification of only 0.5% to 1% per pass. This small amplification necessitates a very high mirror reflectivity of more than 99.5%. Thus, the index contrast between the materials making up the DBR must be as large as possible, while the absorption in the materials must be kept to minimum.

According to our previous calculations [1], double lateral injection or diagonal -current-injection [3] are the only promising electrical schemes at the current stage of technology of nitride VCSELs. Among them, those with both dielectric mirrors require much more advanced technique to be produced than these with AlGaN/AlGaN DBRs. The hybrid solution with one dielectric and one semiconductor mirror may be optimal for CW operating nitride VCSELs. In this section we compare advantages and disadvantages of these approaches. Various materials for resonator DBR mirrors are investigated, namely SiO_2, TiO_2, HfO_2, MgO, Y_2O_3, ZrO_2, Ta_2O_5, GaN, AlN and AlGaN. The results are presented in Fig. 2. We calculated, at room temperature, threshold material gain the fundamental LP_{01} mode for ten considered structures. A detailed explanation of our assumptions for the calculations as well as all material parameters can be found in our previous paper [2]. As one can see, structures with both dielectric DBR mirrors (Nos. 1 – 6) exhibit much less threshold gain (note the logarithmic scale), than those with at least one GaN/AlGaN DBR (Nos. 9 and 10). At the current stage of technology, this difference strongly favours the first ones. Nevertheless, it should be remembered that technological difficulties associated with fabrication of dielectric cavities, especially the necessity of using the lift-off technique [8], could increase their absorption losses.

Among considered structures with both dielectric mirrors, the best results occurred for SiO_2/TiO_2 multilayers. The use of TiO_2 may, however, involve

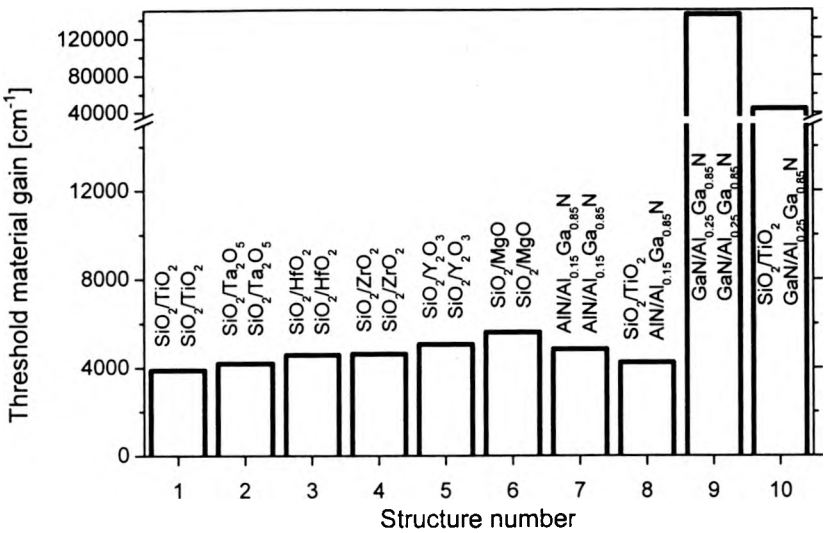

Fig. 2. RT threshold material gain of the fundamental LP_{01} mode for different nitride VCSEL resonator constructions. Alternating structure layers for top and bottom resonator DBRs are indicated. 3λ resonator cavity, 5 μm active-region radius and 5 quantum-well gain region [5] are assumed in the calculations.

unwanted additional processing and optimisation during the electron-beam evaporation to fabricate the low-absorption layer. These difficulties could be roundabout if SiO_2/Ta_2O_5 mirror is used. The absorption coefficient Ta_2O_5 deposited at 250 °C is negligible [11], while the refractive index is still relatively high (2.22) in comparison with that of SiO_2 (1.56). A similarly low threshold gain could be achieved for SiO_2/TiO_2 DBRs as well.

If we replace gallium nitride with aluminium nitride in the nitride DBR mirrors, threshold gain could be significantly reduced. Such a stack of quarter-wavelength $AlN/Al_{0.15}Ga_{0.85}N$ layers is adopted for both DBR mirrors of the 7th structure. The $Al_{0.15}Ga_{0.85}N$ is chosen to ensure a high step change in refractive indices between alternating layers of the DBR structure, while still maintaining limited absorption losses. This material had already been proposed in the literature [12], although serious difficulties with achieving high quality mirrors of that type were also reported [6].

A very low threshold gain is calculated for the 8th structure where the balance between technical difficulties and low threshold material gain seems to be achieved. Moreover AlGaN layers of a bottom DBR (being a part of a heat-sinking path) have much higher thermal conductivity in comparison with dielectric ones, which could be the crucial issue in the case of continuous wave operation of nitride VCSELs. Therefore, while two dielectric SiO_2/TiO_2 DBR mirrors may be recommended for pulsed-operating nitride VCSELs, hybrid mirror structure with the top SiO_2/TiO_2 DBR mirror and the bottom $AlN/Al_{0.15}Ga_{0.85}N$ DBR mirror seems to offer better achievements for continuous-wave operating devices.

3. Active region

The growth of InGaN-based optoelectronics is typically done by metal-organic chemical vapor deposition (MOCVD) on sapphire, yielding dislocation densities of the order of 10^8 cm^{-3}. These dislocations can serve as non-radiative recombination sites, and deteriorate device performance by requiring higher threshold currents for device operation. Fabricating laser structures on laterally epitaxially overgrown (LEO) GaN has been shown to increase device lifetime [13]. In some regions of the active layer fabricated with the help of this technique the dislocation densities may be up to three orders of magnitude lower than in the MOCVD deposition, reaching this way dislocation level of arsenides and phosphides active regions.

At the initial state of nitride technology, it was believed that bulk active region could provide sufficient optical gain for nitride lasers, but it did not occur to be true. Nowadays there are still some reports on light emitting devices based on the bulk nitride active region, but most of these devices and all lasers employ the quantum well active region. Quantum wires and especially quantum dots are expected to reduce threshold current densities [14], but electrically pumped mitride devices based on these types of an active region have not been reported until now at all. Therefore, in this paper, we limit our considerations to a quantum well active region. The mechanism responsible for a very efficient spontaneous light generation in InGaN active region is still puzzling. It is believed that the fluctuation of the indium mole fraction may create traps for electrons and holes efficiently stopping them from non-radiative recombination at dislocations [15]. For small indium mole fraction ($<20\%$), the piezoelectric effect has strong impact on radiative recombination processes. A strong build-in stress originated piezoelectric field separates electrons and holes reducing the probability of radiative recombination, especially in the case of thick quantum wells [16]. A piezoelectric field may be, however, efficiently screened by high concentration of injected carriers and/or high silicon doping of barriers [17]. For a very thin quantum well, surfaces between barriers and a quantum well are more irregular leading to the increase in non-radiative recombination [18].

There are still many unknown issues associated with nitride quantum wells. Thus, in our calculations we decided to use 3.5 nm thick quantum well, frequently applied in efficient commercial nitride LEDs and lasers [19]. The number of quantum wells is limited to 5 due to a possible interwell inhomogeneity of a carrier injection [20]. For the same reason, we assume 10% gain drop in successive wells [21]. To limit carrier escape from the active region, a blocking layer is often used. The layer should have energy gap wider than that of barriers and is usually 20 nm thick. In our calculation we employed $Al_{0.2}Ga_{0.85}N$ for the blocking layer remembering that aluminium atoms diffuse into the active region and additionally increase potential barriers between already localized carriers and thus they increase radiative recombination [22].

An impact of the width of the barriers between quantum wells on threshold material gain was also considered. The RT threshold has been found to increase exponentially with the barrier width (Fig. 3). This could be attributed to the change in the fundamen-

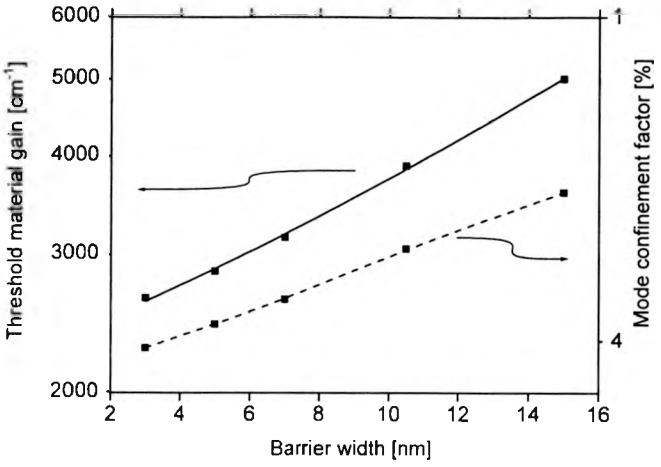

Fig. 3. RT threshold material gain for the structure with both the SiO_2/TiO_2 dielectric mirrors (left axis) and the waveguide direction confinement factor for the resonator (right axis) *vs.* the width of the barriers between quantum wells. The solid and dashed lines represent exponential fit to the simulation data.

tal LP_{01} mode confinement factor in the waveguide direction as is shown in the same figure Increasing the barrier width causes significant decrease in the mode confinement factor. This could be explained if one takes into account the fact that the intensity of the standing wave of the resonator is much lower in the outer quantum wells than in the middle one. Therefore, the gain contribution of outer quantum wells is significantly reduced. Such a behaviour is not so prominent in the case of long wavelength VCSELs.

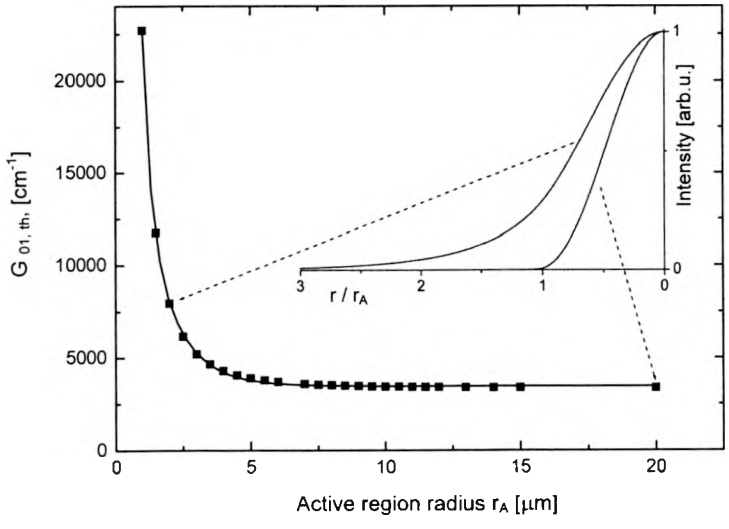

Fig. 4. RT threshold material gain for the VCSEL structure with both the SiO_2/TiO_2 dielectric mirrors *vs.* active region radius. The inset shows radial mode profile for active region radii of 2 μm and 20 μm, respectively.

The active region size was analysed, too. We evaluated the smallest acceptable active region radius, assuming RT fundamental LP_{01} mode laser operation. The results are clearly visible in Fig. 4. For the radius larger than 5 μm, the material gain threshold is almost stable, while for the smaller radius, it starts to increase dramatically. This could be explained by the change in the radial mode profile (see inset in Fig. 4). The smaller the active region radius, the more the mode spreads into a high absorption area and, in this way, increases overall cavity losses and subsequently the threshold gain.

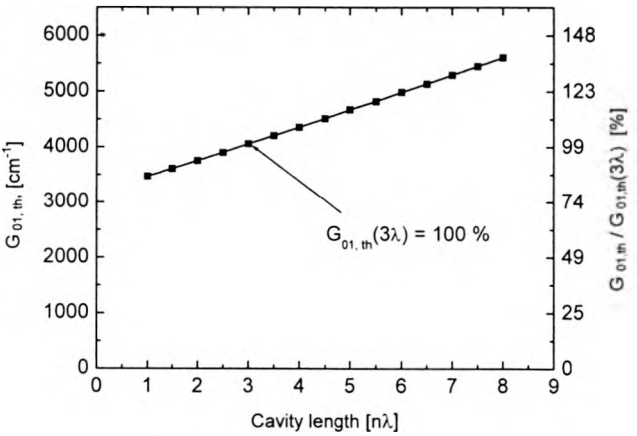

Fig. 5. RT threshold material gain for the VCSEL structure with both the SiO_2/TiO_2 dielectric mirrors *vs.* cavity length (right-hand axis shows relation to the 3λ cavity).

The longitudinal placement of an active region is limited only by the requirement that the active layers should coincide with the maximum intensity of a standing wave of the resonator. However, the overall length of the cavity has great impact on the lasing threshold. Figure 5 presents threshold material gain for different cavity lengths. The threshold gain values are referred to the 3λ cavity construction. It is clearly seen that the shorter cavity, the lower threshold could be achieved. This fact is easy to explain by the decreasing absorption with the decrease in spacer thickness. However it should be remembered that in the double lateral injection scheme, spacers have to be thick enough to ensure efficient current injection in the active region. The spacer thickness would also affect lateral current density and subsequent Joule heat generation. Thus, the optimal thickness of the spacers depends on the applied injection scheme and current densities required to achieve lasing condition. In all cases, however, spacers should be as thin as possible.

4. Current spreading

Nitrides spacers, apart from their optical function, play very important role in current spreading. They are usually made of gallium nitride but AlGaN/GaN

superlattices are also of great interest. In the case of standard p-type GaN, the lateral electrical conductivity is not sufficient to compete with vertical transport until the device area approaches approximately 1 μm. Such a small optical aperture in turn implies prohibitive transverse modal losses for a VCSEL (*cf.* Fig. 4). Therefore, when a double lateral injection scheme is applied, highly non-uniform carrier-concentration profiles are formed. The carrier density, being practically insignificant within the central circular part of active regions, is increasing dramatically when approaching the active-region perimeter. Subsequently, material gain non-uniformity strongly favours unwanted higher-order transverse modes. Additionally, the temperature profile with a distinct maximum at the edge of active region results in such changes of refractive indices that strong anti-guiding effect is trying to shift modes outside the active region. Furthermore, it should be remembered that technological processes associated with formation of current confinement region could create centers of non-radiative recombination at the edges of the active region.

Uniformity of carrier injection may be improved by introducing a semitransparent electrical contact into the cavity [9], [23], [24], or the application of a tunnel junction [24]–[26]. These approaches can be used simultaneously. They both distribute injected carriers in an active region in a more uniform fashion and compensate very short diffusion length of carriers in nitrides.

A resonant-cavity nitride LED with semitransparent contact and a tunnel junction has already been demonstrated [24]. However, a VCSEL is still beyond the reach of this solution. According to our calculations, it is due to high absorption losses associated with a semitransparent indium tin oxide (ITO) layer used in the constructions. The thickness of the semitransparent contact occurred to be crucial for a successful construction. The ITO contact should be as thin as possible and, to minimize optical losses, placed in the node of a standing wave of the resonator. There are reports on fabrication of 25 nm ITO contacts with a very low absorption of 664 cm^{-1} [27]. A semitransparent contacts of these parameters may be very useful in forming current distribution, especially when a properly deposited ITO contact additionally forms a current confinement [24].

The use of a tunnel junction results in replacing most of the p-type GaN spacers with the n-type material of much better electrical conductivity. Additionally, both contacts may be of n-type having distinctly lower sheet resistance. The other advantage of using a tunnel junction is the possibility of confining the current flow by selective etching of a tunnel junction and re-growth of a nitride structure (buried tunnel junction) [28]. It is also possible to create multiple active regions, when tunnel junctions are employed [29].

If neither a tunnel junction nor a semitransparent contact is used in the nitride VCSEL construction, the main obstacle for successful current injection into the active region is formation of a current confinement. The n-type and the p-type contacts have to be separated by the high resistive region beyond the central VCSEL part (see Fig. 1). To form such a high resistive region, $^2H^+$ ion implantation could be used. The implantation may be performed across the n-type spacer, as the following

thermal annealing would restore initial, preimplanted electrical resistance of the n-type GaN [30], leaving the part of the p-type spacer highly resistive. Also low-energy electron beam irradiation or wet oxidation, similar to the one used to create insulating material in GaAs-based VCSELs, are believed to be alternatively used [23]. A selective lateral etching [31] or selective-area epitaxial re-growth [32] may be employed for that purpose as well. Although so many techniques may be used to form selectively high resistive region, none of them proved its usability and is far from being so efficient and easy to apply as an oxidation of AlAs layers in the case of arsenides lasers.

5. Summary

The main goal of the present work is to present technological difficulties and complexity of designing processes associated with nitride VCSELs. We performed numerical simulations of possible nitride VCSEL configurations. For pulse-operating nitride VCSELs, both dielectric resonator mirrors (preferably SiO_2/TiO_2 or SiO_2/Ta_2O_5 stacks) are recommended, whereas in the case of continuous-wave operation, the bottom dielectric mirror should be replaced by the semiconductor one (*e.g.*, $GaN/Al_{0.15}Ga_{0.85}N$ stack) to enhance heat extraction. It is shown that the active region radius in the analysed lasers should not be less than 5 μm. We also analysed difficulties associated with an efficient current confinement and carrier injection into the active region. Our considerations cover the application of a tunnel junction and a semitransparent contact in nitride VCSELs.

Acknowledgments — This work was supported by the State Committee for Scientific Research (KBN), Poland, grants No. 7T11B06920 and No. 7T11B 073 21.

References

[1] MAĆKOWIAK P., NAKWASKI W., J. Phys. D: Appl. Phys. **33** (2000), 642.
[2] MAĆKOWIAK P., NAKWASKI W., J. Phys. D: Appl. Phys. **34** (2001), 954.
[3] MAĆKOWIAK P., SARZAŁA R. P., NAKWASKI W., Semicond. Sci. Technol. **16** (2001), 598.
[4] SARZAŁA R. P., MAĆKOWIAK P., NAKWASKI W., Semicond. Sci. Technol. **17** (2002), 255.
[5] PARK S.-H., CHUANG S.-L., Appl. Phys. Lett. **72** (1998), 287.
[6] NG H. M., MOUSTAKAS T. D., CHU S. N. G., Appl. Phys. Lett. **76** (2000), 2818.
[7] WALDRIP K. E., HAN J., FIGEL J. J., ZHOU H., MAKARONA E., NURMIKKO A. V., Appl. Phys. Lett. **78** (2001), 3205.
[8] WONG W. S., KNEISSEL M., MEI P., TREAT D. W., TEEPE M., JOHNSON N. M., Jpn. J. Appl. Phys. Pt. 2, **39** (2000), L1203
[9] SONG Y.-K., DIAGNE M., ZHOU H., NURMIKKO A. V., SCHNEIDER R. P., Jr, TAKEUCHI T., Appl. Phys. Lett. **77** (2000), 1744.
[10] DUDLEY J. J., BABIĆ D. I., MARTIN R. P., YANG L., MILLER B. I., RAM R. J., REYNOLDS T. E., HU E. L., BOWERS J. E., Appl. Phys. Lett. **64** (1994), 1463.
[11] MARGALITH T., ABARE A. C., BUCHINSKY O., COHEN D. A., HANSEN M., STONAS A. R., MACK M. P., HU E. L., DENBAARS S. P., COLDREN L. A., Proce. SPIE **3944** (2000), 10.
[12] IGA K., Electron. Commun. Jap. Pt. 2, **82** (1999), 70.

[13] NAKAMURA S., SENOH M., NAGAHAMA S., IWASA N., YAMADA T., MATSUSHITA T., KIYOKU H., SUGIMOTO Y., KOZAKI T., UMEMOTO H., SANO M., CHOCHO K., Appl. Phys. Lett. **72** (1998), 211.
[14] HUANG W., JAIN F., J. Appl. Phys. **87** (2000), 7354.
[15] CHO Y.-H., SCHMIDT T.J., FISCHER A.J., BIDNYK S., GAINER G.H., SONG J.J., KELLER S., MISHRA U.K., DENBAARS S.P., KIM D.S., JHE W., Phys. Status Solidi B **216** (1999), 181.
[16] SHAPIRO N.A., FEICK H., GARDNER N.F., GOETZ W.K., WALTEREIT P., SPECK J.S., WEBER E.R., Phys. Status Solidi B **228** (2001), 147.
[17] SHAPIRO N.A., PERLIN P., KISIELOWSKI C., MATTOS L.S., YANG J.W., WEBER E R., MRS Internet J. Nitride Research **5** (2000), Article 1.
[18] GAINER G.H., KWON Y.H., LAM J.B., BIDNYK S., KALASHYAN A., SONG J.J., CHOI S C., YANG G.M., Appl. Phys. Lett. **78** (2001), 3890.
[19] NAKAMURA S., IEEE J. Selected Topics Quantum Electron. **3** (1997), 712.
[20] DOMEN K., SOEJIMA R., KURAMATA A., HORINO K., KUBOTA S., TANAHASHI T., Appl. Phys. Lett. **73** (1998), 2775.
[21] TESSLER N., EISENSTEIN G., IEEE J. Quantum Electron. **29** (1993), 1586.
[22] LEFEBVRE P., TALIERCIO T., MOREL A., ALLEGRE J., GALLART M., GIL B., MATHIEU H., DAMILANO B., GRANDJEAN N., MASSIES J., Appl. Phys. Lett. **78** (2001), 1538.
[23] OSIŃSKI M., SMAGLEY V.A., FU CH.-SH., SMOLYAKOV G.A., ELISEEV P.G., SPIE Proc. **3944** (2000), 3944.
[24] DIAGNE M., HE Y., ZHOU H., MAKARONA E., NURMIKKO A.V., HAN J., WALDRIP K.E., FIGIEL J.J, TAKEUCHI T., KRAMES M., Appl. Phys. Lett. **79** (2001), 3720.
[25] JEON S.R., SONG Y.-H., JANG H.J., YANG G.M., HWANG S.W., SON S.J., Appl. Phys. Lett. **78** (2001) 3265.
[26] TAKEUCHI T., HASNAIN G., CORZINE S., HUECHEN M., SCHNEIDER R.P., Jr, KOCOT CH., BLOMQVIST M., CHANG Y., LEFFORGE D., KRAMES M.R., COOK L.W., STOCKMAN S.A., Jpn. J. Appl. Phys. Pt. 1, **40** (2001), L861.
[27] MARGALITH T., BUCHINSKY O., COHEN D.A., ABARE A.C., HANSEN M., DENBAARS S.P., COLDREN L.A., Appl. Phys. Lett. **74** (1999), 3930.
[28] JEON S.-R, OH CH. S., YANG J.-W., MO YANG G., YOO B.-S., Appl. Phys. Lett. **80** (2002), 1933.
[29] UCHIJAMA S., IGA K., IEEE J. Quantum Electron. **22** (1986), 302.
[30] PEARTON S.J., WILSON R.G., ZAVADA J.M., HAN J., SHUL R.J., Appl. Phys. Lett.. **73** (1998), 1877.
[31] STONAS A.R., MARGALITH T., DENBAARS S.P., COLDREN L.A., HU E.L., Appl. Phys. Lett. **78** (2001), 1945.
[32] KURAMOTO M., KIMURA A., SASAOKA CH., ARAKIDA T., NIDO M., MIZUTA M., Jpn. J. Appl. Phys. Pt. 2, **40** (2001), L925.

Received May 13, 2002